ELSEVIER

www.elsevier.nl/locate/jorganchem

Journal of Organometallic Chemistry 609 (2000) 36–43

Journal of Organometallic Chemistry

An intramolecular N–H···Co hydrogen bond and a structure correlation study of the pathway for protonation of the $Co(CO)_3L^-$ anion (L = CO, PR_3)

Lee Brammer *, Juan C. Mareque Rivas, Christopher D. Spilling

Department of Chemistry, University of Missouri-St. Louis, 8001 Natural Bridge Road, St. Louis, MO 63121-4499, USA

Received 25 April 2000; received in revised form 6 June 2000

Abstract

A low temperature X-ray crystal structure of the zwitterionic organometallic compound $Co(CO)_3\{PPh_2(C_6H_4NHMe_2)\}$ (**2**) provides the first example of an intramolecular N–H···Co (d^{10}) hydrogen bond. Synthesis and characterization of such intramolecularly hydrogen-bonded systems have proven much more elusive than their counterparts that exist as intermolecularly hydrogen-bonded salts. The molecular structure of **2** taken together with a series of previously characterized N–H···M (d^{10}) hydrogen-bonded salts provides a series of snapshots of the changes in geometry at the metal center as one progresses along the pathway for protonation of the anion $Co(CO)_3L^-$ (L = CO, PR_3) to yield the metal hydride $HCo(CO)_3L$.

Keywords: Structure correlation study; Protonation pathway; Intramolecular N–H···Co bond

1. Introduction

Over the past decade in particular there has been an emergence of research concerning an array of hydrogen bond types variously categorized as 'weak' or 'non-conventional' [1], the archetype of which is the C–H···O hydrogen bond [2]. A class of non-conventional hydrogen bonds that arises only in inorganic systems, notably within organometallic and coordination chemistry, is the D–H···M [3,4] hydrogen bond (D = hydrogen bond donor, A = hydrogen bond acceptor, M = transition metal). In earlier work we have established spectroscopic, geometric and chemical criteria for identifying D–H···M hydrogen bonds [3a,d]. In many respects they resemble conventional hydrogen bonds. An important difference arises when one considers the hydrogen bond as an incipient proton transfer reaction. In a conventional hydrogen bond, D–H···A, the hydrogen atom is protonic in nature before, during and after transfer from hydrogen bond donor to acceptor. Indeed, the reverse hydrogen bond D···H–A may be able to form. By contrast, proton transfer arising from a D–H···M hydrogen bond results in a metal hydride species (M–H) that is unable to form the reverse hydrogen bond, D···H–M [5], due to the hydridic nature of the hydrogen atom. Much of our own work in this area has involved the study of N–H···Co hydrogen bonds in salts of the type $R_3NH^+Co(CO)_3L^-$ (L = CO [3b,c,e,g], triarylphosphine [3e,f]). Consistent with the above comments, and pertinent to our own work, is the observation by Norton, Sweany and co-workers that, despite its notable thermodynamic acidity, $HCo(CO)_4$ does not form Co–H···A hydrogen bonds [6]. A further distinction between D–H···M hydrogen bonds and more conventional hydrogen bonds is evident when one considers the contributions to the hydrogen bond energy. A recent report describes ab initio (MP2 level) calculations on O–H···PtL_4 hydrogen bonds and suggests that, in contrast to conventional hydrogen bonds, there is a substantial dispersion contribution to the hydrogen bond energy [4n]. Our own ab initio calculations on a variety of D–H···M hydrogen bonds suggest a greater polarization contribution than is present in conventional hydrogen bonds [7].

* Corresponding author. Tel.: +1-314-5165345; fax: +1-314-5165342.

E-mail address: lee.brammer@umsl.edu (L. Brammer).

0022-328X/00/$ - see front matter
PII: S0022-328X(00)00377-6

In earlier work on hydrogen-bonded R_3NH^+ $Co(CO)_3L^-$ salts, the focus was entirely on intermolecular hydrogen bonds [3b,c,e,f]. The present report describes efforts to prepare an intramolecularly hydrogen-bonded analog of these systems. While intramolecular D–H···M hydrogen bonds are known for square planar d^8 metal centers [4c,d,f,g] and for d^6 metallocarbinols [4h–j], prior to this report there had been only one such example involving a tetrahedral d^{10} metal center [4b]. Here we report the reaction of an N,P-chelating ligand $PPh_2(o\text{-}C_6H_4CH_2NMe_2)$ **1** with $HCo(CO)_4$ in which displacement of a CO ligand by the phosphine coupled with transfer of the metal-bound hydrogen to the amine yields the desired hydrogen-bonded system, **2**, which has been characterized by low temperature X-ray diffraction.

Accumulated structural data on a series of N–H···Co hydrogen-bonded salts, including **2**, have then been used to map out the reaction pathway for protonation of the $Co(CO)_3L^-$ anion to yield the hydride complex $HCo(CO)_3L$ (L = CO, PR_3).

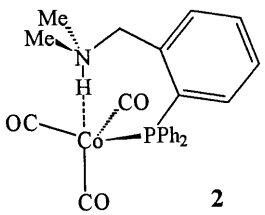

2

2. Experimental

2.1. General synthetic procedures and instrumentation

All manipulations of oxygen- and/or water-sensitive materials were carried out under an atmosphere of argon either using Schlenk-line techniques or in a Vacuum Atmospheres drybox. NMR spectra were recorded on a Varian Unity-Plus 300 MHz or Bruker ARX-500 spectrometer.

2.2. Synthesis of *o*-diphenylphosphino-*N*,*N*-dimethylbenzylamine (*1*)

Following literature precedent [8], to a stirring solution of *n*-BuLi in hexanes (2.5 M, 12 ml, 0.03 mol) at r.t. was added dimethylbenzylamine (3.75 ml, 0.025 mol). The reaction mixture was diluted with freshly distilled Et_2O (38 ml) and allowed to stand for 24 h. The lithiated benzylamine deposited on the flask as a mass of yellow crystals leaving an orange solution. The crystalline mass was re-suspended in solution with vigorous stirring. The solution was cooled in an ice water bath and diphenylchlorophosphine (5.4 ml, 0.03 mol) was added slowly. The reaction mixture was stirred for an additional hour in the ice bath and then was allowed to warm to r.t. (20 min). The mixture was re-cooled in ice and the reaction was cautiously quenched by the slow addition of a large excess of water (5 ml). The reaction mixture was partitioned between 2 M HCl (100 ml) and Et_2O (100 ml). The Et_2O was re-extracted with HCl (100 ml) and the combined HCl extracts were adjusted to pH 12 with NaOH. The resulting aqueous solution was extracted with CH_2Cl_2 (3 × 75 ml) and the combined extracts were dried, filtered and evaporated in vacuo to give an orange oil. (7.53 g, 94%). ^{31}P-NMR δ −14.6 p.p.m. indicates 95% purity in accord with a previous literature report [9b]. The X-ray crystal structure of the salt **1**·HCl has been determined, but will be reported elsewhere.

2.3. Synthesis of $Co(CO)_3\{PPh_2(o\text{-}C_6H_4CH_2NHMe_2)\}$ (*2*)

$Co_2(CO)_8$ (1.52 g, 4.4 mmol) was dissolved in hexane (35 ml) and to the stirring solution at r.t. an excess of dimethylformamide (8 ml) was added. For 1 h the mixture was stirred after which two layers appeared, a colorless upper layer and a pink lower layer. The solution was then cooled to −78°C and 8 ml of 1 M HCl was slowly added. After addition was completed the mixture was allowed to warm to 0°C and stirred for 20 min. After that time, the organic layer turned yellow ($HCo(CO)_4$) and the aqueous layer blue ($CoCl_2$). The aqueous layer was removed and the yellow solution was washed with two equal portions of water (10 ml) and afterwards dried over P_2O_5 at −78°C for 30 min. The dried solution containing $HCo(CO)_4$ was slowly added to a solution of **1** (1.4 g, 4.4 mmol) in toluene (15 ml) at −196°C. After the addition was completed, the mixture was allowed to warm to −78°C and stirred for 15 min, yielding an orange solution and orange precipitate. The orange solution was transferred to another flask and slow evaporation overnight yielded yellow crystals of **2** suitable for X-ray diffraction, during which time the solution turned red.

The orange precipitate was dried under vacuum to give an orange solid. This solid contained a mixture of species, which proved impossible to separate. ^{1}H-NMR data for this material in $C_6D_5CD_3$ revealed resonances indicative of N–H protons (in the range δ 10–14), suggesting the possible presence of **2** together with other related products. Dissolution of the yellow crystals of **2** repeatedly yielded NMR spectra consistent only with the ligand **1**. Ultimately, definitive spectroscopic characterization of **2** did not prove feasible, despite numerous repetitions of the synthesis. One common by-product, the red dimer $[Co(CO)_3\text{-}\{PPh_2(o\text{-}C_6H_4CH_2NMe_2)\}]_2$ (**3**) with monodentate phosphine-bound ligands, was later identified and crystallographically characterized. The analogous by-

product, $[Co(CO)_3(PPh_3)]_2$, was observed in earlier work using PPh_3 in the preparation of $(DABCO)H^+$ $Co(CO)_3PPh_3^-$ (DABCO = 1,4-diazabicyclooctane) [3e].

2.4. X-ray crystal structure determination of $Co(CO)_3\{PPh_2(o\text{-}C_6H_4CH_2NHMe_2)\}$ (2)

Crystalline compound **2** decomposes rapidly in air. Thus, crystals were first coated in hydrocarbon oil in the drybox, and subsequently mounted on glass fibers and rapidly transferred to the cold nitrogen stream of the diffractometer. A number of intensity data sets were collected on different crystals of **2** using a Bruker SMART CCD-based area detector diffractometer. The refinement based upon the best of these data sets is presented herein. However, even the best data set obtained was from a crystal that exhibited unresolved twinning. As efforts to obtain an accurate description of the twinning were unsuccessful, the intensity data were integrated so as to minimize the effects of twinning. Thus, a single orientation matrix that was a very good fit to the positions of 500 diffraction maxima associated with the major twin component was obtained. This matrix was used for integration of the full data set without further refinement of the matrix during integration. Symmetry-equivalent data showing poor internal agreement in intensity were examined by hand. For these groups of reflections, either the outliers or the entire set of symmetry-equivalent reflections were removed. A total of 371 reflections were thus eliminated. No absorption correction was applied. A weighting scheme was chosen to provide an approximately constant analysis of variance across all groups of reflections and to downweight the contribution of the weakest reflections, a number of which are somewhat overestimated in intensity due to the residual effects of the twinning. The oxygen atom displacement parameters were constrained to be 1.4 times that of the attached carbonyl carbons, and the distances in ring C(11)–C(16) were restrained to have mutually similar displacement parameters. Hydrogen atoms were included in calculated positions with fixed isotropic displacement parameters, and refined using a riding model. All other non-hydrogen atoms were refined freely with anisotropic displacement parameters. Refinement converged to a sensible geometry with physically reasonable anisotropic displacement parameters. Thus, despite somewhat low data quality for **2**, the use of appropriate refinement methods has led to structure determination of adequate accuracy for unambiguous identification of **2**, and discussion of its geometry with modest precision. The crystal structure was solved by direct methods and refined to convergence against F^2 data [$F^2 \geq -3\sigma(F^2)$] using the SHELXTL suite of programs [9]. Further experimental details are provided in Table 1 and in CIF format as supplementary data.

Table 1
Data collection, structure solution, and refinement parameters for **2** and **3** [a]

	2	**3**
Crystal color	Yellow	Red
Crystal size (mm)	$0.33 \times 0.30 \times 0.03$	$0.08 \times 0.07 \times 0.03$
Crystal system	Triclinic	Monoclinic
Space group, Z	$P\bar{1}$, 2	$P2_1/n$, 2
a (Å)	7.9437(1)	10.590(9)
b (Å)	8.0781(1)	15.513(13)
c (Å)	18.1070(1)	14.052(11)
α (°)	98.437(1)	90
β (°)	100.579(1)	101.36(2)
γ (°)	98.241(1)	90
V (Å^3)	1112.36(3)	2263(3)
D_{calc} (g cm^{-3})	1.383	1.357
Temperature (K)	133(5)	208(5)
μ(Mo–K$_\alpha$) (mm^{-1})	0.868	0.853
θ range (°)	1.16–25.00	1.98–25.00
Reflections collected	11409	29628
Independent reflections, n, (R_{int})	3922 (0.093)	3988 (0.149)
Reflections used in refinement	3551	3963
L.S. parameters (p)	253	271
Restraints (r)	15	0
$R_1(F)$ [b], $[I>2.0\sigma(I)]$	0.172	0.083
$wR_2(F^2)$ [b], all data	0.441	0.170
$S(F^2)$ [b], all data	1.18	1.36

[a] Esds in cell parameters for **2** are unrealistically small due to the large number of data used in the calculation. These values represent random and not systematic errors in the parameters.

[b] $R_1(F) = \Sigma(||F_o| - |F_c||)/\Sigma|F_o|$; $wR_2(F^2) = [\Sigma w(F_o^2 - F_c^2)^2/\Sigma wF_o^4]^{1/2}$; $S(F^2) = [\Sigma w(F_o^2 - F_c^2)^2/(n-p)]^{1/2}$.

2.5. X-ray crystal structure determination of $[Co(CO)_3\{PPh_2(o\text{-}C_6H_4CH_2NMe_2)\}]_2$ (3)

In the solid state this compound decomposes only over prolonged exposure to air (days). However, as a precaution, crystals were first coated in hydrocarbon oil in the drybox, and subsequently mounted on glass fibers and rapidly transferred to the cold nitrogen stream of the diffractometer. The intensity data set for **3** was collected using a Bruker SMART CCD-based area detector diffractometer. An absorption correction was applied using empirical methods [10] based upon the method of Blessing [11].

The crystal structure was solved by direct methods and refined to convergence against F^2 data [$F^2 \geq -3\sigma(F^2)$] using the SHELXTL suite of programs [9]. All non-hydrogen atoms were refined anisotropically. Hydrogen atoms were included in calculated positions with fixed isotropic displacement parameters, and refined using a riding model. Further experimental details are

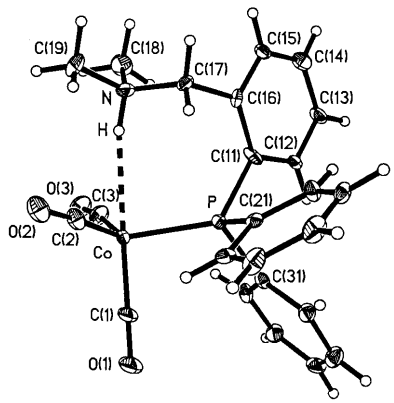

Fig. 1. Molecular structure of **2** shown with 30% probability ellipsoids for non-hydrogen atoms.

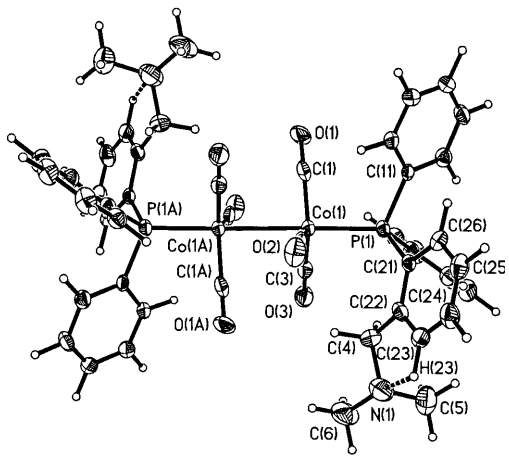

Fig. 2. Molecular structure of **3** shown with 30% probability ellipsoids for non-hydrogen atoms.

provided in Table 1 and in CIF format as supplementary data.

3. Results and discussion

3.1. Crystal structures of *2* and *3*

The molecular structures of **2** and **3** are shown in Figs. 1 and 2, respectively. Crystallographic data are summarized in Table 1 and selected interatomic distances and angles are provided in Table 2.

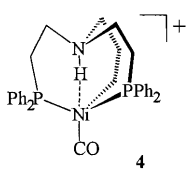

4

The molecular structure of **2** provides the second example of an intramolecular N–H···M hydrogen bond involving a tetrahedral d^{10} metal center, the first for Co(–I). The previous example, [Ni{NH($CH_2CH_2PPh_2$)$_3$}CO]BPh_4 (**4**), reported by Midollini and coworkers [4b], was not explicitly described by the authors as having an N–H···Ni hydrogen bond, but exhibits all the hallmarks of analogous interactions involving d^{10} Co centers [3b,c,e,f, 4a], including **2**. Indeed, extended Hückel calculations reported for **4** suggest an electrostatic component to the N–H···Ni interaction is important (as is typical of a hydrogen bond). The hydrogen bond [N···Co, 3.31(2); H···Co, 2.27 Å; N–H···Co, 166.1°] [12] in **2** is longer than that in **4** [N···Ni, 3.098(8); N–H 1.15(9); H···Ni, 1.95(9) Å; N–H···Ni, 171(6)°], consistent with the fact that three carbon atoms separate the nitrogen and phosphorus in **2**, but only two carbon atoms provide the link in **4**. The hydrogen bond in **2** is similar in geometry to that of the intermolecular hydrogen bonds in (DABCO)H^+ $Co(CO)_3PPh_3^-$ (**5**) [3.294(6), 2.25 Å, 169.6°] [3e, 12], [(DABCO)H^+][$Co(CO)_3PPh_2$(*p*-tol)$^-$]·CH_3CN **6**·CH_3CN [3.347(6), 2.30 Å, 175.5°] [3f, 12] and [(DABCO)H^+][$Co(CO)_3P$(*p*-tol)$_3^-$]·CH_3CN **7**·CH_3CN [3.371(2), 2.32 Å, 177.4°] [3f, 12] (*p*-tol = *para*-tolyl). However, while the phosphine lies *trans* to the hydrogen bond in **5**–**7**, a *cis* arrangement, of course, facilitates the intramolecular hydrogen bond in **2**. In **5**–**7**, the nitrogen substituents of the ammonium cation are typically staggered about the hydrogen bond with respect to the (equatorial) carbonyl ligands of the anion (torsion angle C–N···Co–C of ca. 60° [13]), whereas in **2** the constraint of the intramolecular hydrogen bond results in a mean C–N···Co–L torsion angle of only 16°. Similarly, in **5**–**7**, the $(OC)_3Co$ and PR_3 moieties are

Table 2
Selected interatomic distances (Å) and angles (°) for **2** and **3** [a]

	2	**3**
Co–Co		2.702(2)
Co–P	2.194(5)	2.218(2)
Co–C(1) [b]	1.75(2)	1.798(8)
Co–C(2)	1.76(2)	1.799(8)
Co–C(3)	1.71(2)	1.766(8)
Co···N	3.31(2)	
C(1)–O(1) [b]	1.13(3)	1.153(7)
C(2)–O(2)	1.16(2)	1.153(7)
C(3)–O(3)	1.19(2)	1.160(7)
P–C(11)	1.84(2)	1.827(6)
P–C(21)	1.83(2)	1.852(6)
P–C(31)	1.87(2)	1.833(6)
P–Co–C(1)	95.7(8)	96.1(2)
P–Co–C(2)	115.4(6)	93.1(2)
P–Co–C(3)	112.9(7)	95.7(2)
C(1)–Co–C(2)	104.7(10)	119.5(3)
C(1)–Co–C(3)	109.0(12)	118.0(3)
C(2)–Co–C(3)	116.5(9)	120.3(3)

[a] For compound **3**, label Co corresponds to atoms Co(1) and/or Co(1a) in Fig. 2 and label P corresponds to atom P(1) Fig. 2.
[b] Axial CO in **2**.

staggered about the Co–P bond, whereas in **2**, the intramolecular hydrogen bond constrains this torsion angle to ca. 28° (mean of three C–Co–P–C angles). No significant differences between **2** and **5**–**7** in Co–C, Co–P or C≡O distances are observed.

A common decomposition pathway for $HCo(CO)_3L$ ($L = CO$, PR_3) leads to formation of the symmetric Co–Co bonded dimer $Co_2(CO)_6L_2$ [14], as we have observed previously for $L = PPh_3$ [3e]. We were able to crystallographically characterize the corresponding dimer, **3**, where $L = PPh_2(o\text{-}C_6H_4CH_2NHMe_2)$ (**1**). The two phosphine ligands are coordinated in a monodentate manner through phosphorus, and lie *trans* to the Co–Co bond. This is consistent with all previously reported structures of $Co_2(CO)_6L_2$ dimers, where L is a monodentate ligand [15]. Interestingly the benzyl amine group in **3**, bearing an unprotonatated nitrogen, adopts a conformation in which the amine nitrogen lies approximately in the plane of the aryl ring [C(23)–C(22)–C(4)–N(1) −23.3 versus C(15)–C(16)–C(17)–N 100.2° in **2**]. This conformation facilitates an intramolecular C–H···N hydrogen bond (Fig. 2), which satisfies the hydrogen bond acceptor capability of the amine nitrogen [H···N 2.306 Å and C–H···N 101.8°, using C–H 1.083 Å]. Metal–metal and metal–ligand bonds in **3** are similar to, but slightly longer than those of (six) related structures [15], viz. Co–Co 2.645–2.671, cf. 2.702(2) Å in **3**, Co–P 2.135–2.178, cf. 2.218(2) Å in **3**, and Co–C 1.754–1.774, cf. 1.788 Å (average) in **3**.

3.2. Spectroscopic characterization of *2*

As noted in the experimental section, spectroscopic characterization of **2** proved elusive in contrast to the intermolecularly hydrogen-bonded analogs **5**–**7**, despite numerous attempts to obtain NMR or IR data on the pure material. Typical ^{1}H-NMR data (in toluene-d_8) for the crude product showed a number of resonances in the region δ 10–14, consistent with N–H groups, but indicative of more than one product, and inconclusive in identifying **2**. NMR spectra obtained from dissolution of the crystals of **2** (in toluene-d_8) were consistent only with the presence of the ligand, **1**. IR data, for which the ν(CO) stretches have been valuable in characterizing previous intermolecularly hydrogen bonded systems **5**–**7**, did not exhibit a pattern of carbonyl bands consistent with either **2** or likely by-products, but suggested a mixture of carbonyl containing products.

These observations suggest considerable instability of **2** relative to **5**–**7**, in particular indicating that aminophosphine loss from **2** is quite facile in solution. In this light the definitive crystallographic characterization of **2** is all the more remarkable. In an effort to obtain species similar to **2**, but with greater stability, two other aminophosphines, Ph_2Ppy (py = 2-pyridyl) (**8**), $Ph_2PCH_2CH_2NEt_2$ (**9**), were prepared and reacted with $HCo(CO)_4$ as per the procedure described for the preparation of **2**. In both cases the product strongly implicated from ^{1}H-NMR data (doublet at ca. δ −10) was the monophosphine-hydride compound, $HCo(CO)_3L$ ($L =$ **8** or **9**). No evidence for the formation of N–H···Co hydrogen-bonded products was found. The likely explanation is either the nitrogen is not basic enough (**8**) to be protonated by $HCo(CO)_3L$ or the phosphine is so electron donating that the hydride ligand is less easily deprotonated by the amine base (**9**). Of course, these explanations amount to the same result, but provide a different emphasis.

3.3. Pathway for protonation of the anion $Co(CO)_3L^-$ ($L = CO$, PR_3)

An instructive way to think of a hydrogen bond is as an incipient proton transfer. This provides a link between structure and reaction, protonation in this case. Taken collectively, the crystal structures of **2**, **5**–**7** and other $R_3NH^+Co(CO)_4^-$ structures provide a series of snapshots of the protonation of the $Co(CO)_3L^-$ anion by an ammonium cation, R_3NH^+. Arranging these molecular structures sequentially one can use the Structure Correlation Principle [16] to map out the reaction pathway in terms of the changes in geometry of the $R_3NH^+Co(CO)_4^-$ unit. In this case it is most instructive to follow the change in geometry around the metal center as a function of H···Co separation. The former is most readily quantified in terms of the mean L_{eq}–Co–L_{eq} or L_{ax}–Co–L_{eq} angles, where L_{eq} and L_{ax} are the equatorial and axial ligands most readily defined in the pseudo-trigonal bipyramidal geometry of the metal hydride product of protonation, $HCo(CO)_3L$. In addition to the N–H···Co hydrogen-bonded structures, the initial point of the reaction pathway is represented by ammonium and $Co(CO)_3L^-$ ions situated at approximately van der Waals separation [H···Co 3.0 Å]. The metal hydride endpoint of the protonation reaction is represented by the structures of $HCo(CO)_4$ [17], $HCo(CO)_3L$ (known only for $L = PCy_3$ [18]) and the isoelectronic d^{10} anion present in $PPN^+HFe(CO)_4^-$ [19], the latter being isoelectronic and structurally similar to $HCo(CO)_4$. Data for the more constrained, and intramolecularly N–H···Ni hydrogen-bonded, system, **4**, again involving a d^{10} metal center, are also included in the analysis. Scheme 1 depicts all structures, shown sequentially, together with pertinent geometric data. Fig. 3 shows the Structure Correlation analysis of the protonation pathway [20].

A number of important points arise from examination of the Structure Correlation plot (Fig. 3). The geometric changes that occur over the course of the protonation reaction can be followed along either of the solid lines, which although fitted mathematically to

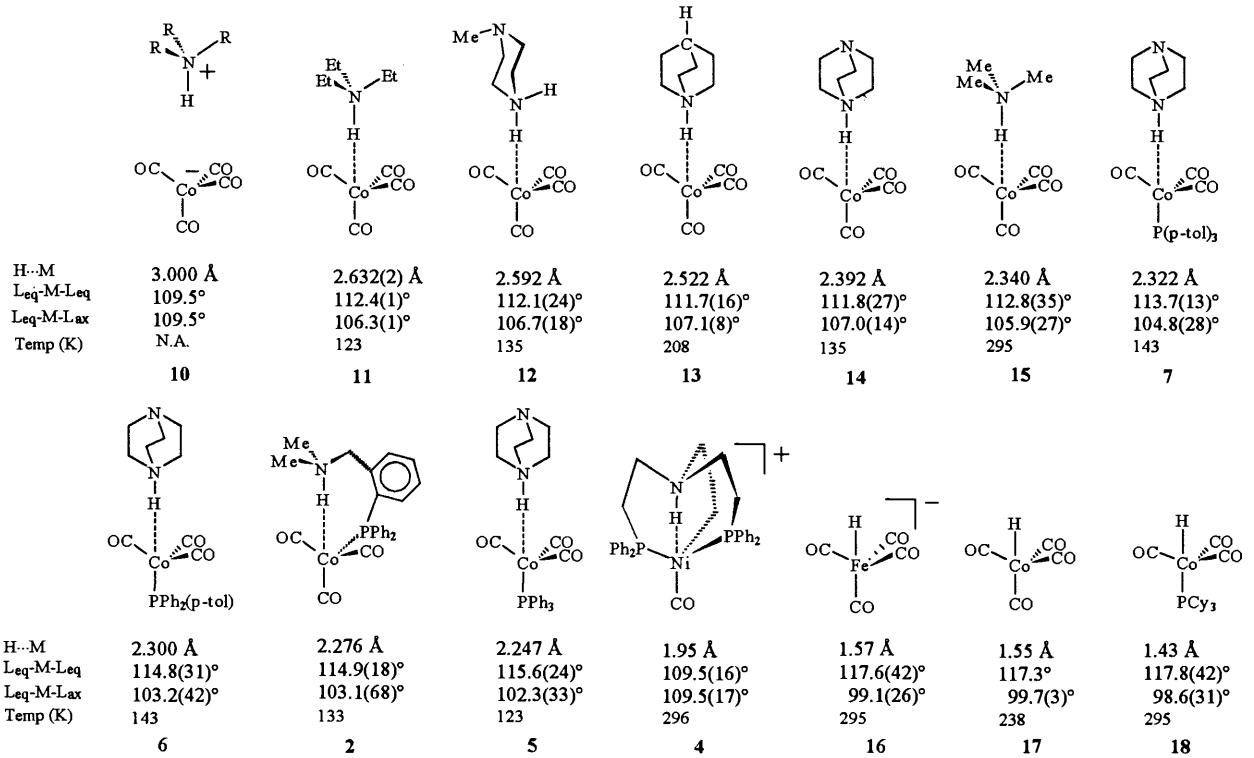

Scheme 1. Structures whose geometries were used in the Structure Correlation study to determine the geometric changes that define the pathway for protonation of $Co(CO)_3L^-$. Average values $\langle r \rangle$ are listed for the angles with esds (σ) representing the scatter in these angles (i.e. $\sigma = [\Sigma_i(\langle r \rangle - r_i)^2/(n-1)]^{1/2}$, where $r_i = i$th observation, $n =$ number of observations). These e.s.d.s do not necessarily correlate with those of individual angles. H–M distances for **12**–**15**, **7**, **6**, **2**, and **5** are calculated after normalizing the X-ray determined N–H distance to 1.054 Å, as determined by neutron diffraction in **11**. Original references for the X-ray structures are **10** [model geometry, this work], **11** ([21], neutron diffraction), **12** [3c], **13** [3e], **14** [3f], **15** [4a], **7** [3f], **6** [3f], **2** (this work), **5** [3e], **4** [4b], **16** [19], **17** ([17], electron diffraction), **18** [18]. See also Ref. [22] for reports of the synthesis and IR characterization, but not crystal structures, of $HCo(CO)_3PPh_3$, $HCo(CO)_3P(OPh)_3$ and Et_3NH^+ $Co(CO)_3PPh_3^-$.

the data points should be used primarily to guide the eye in interpreting the plot. Progression along the reaction pathway (right to left) may be described as follows. Approach of the N–H group of the cation to one face of the tetrahedral anion and formation of the N–H···Co hydrogen bond results initially in little perturbation of the metal coordination geometry. Thus, by the time that the H···Co separation has decreased to ca. 2.4, from the approximately 3.0 Å at van der Waals separation [23], the interligand angles have changed relatively little from 109.5 to L_{eq}–Co–L_{eq} 112 and L_{ax}–Co–L_{eq} 107°, typified by the structure of **14**. This corresponds to a slight opening up of the anion geometry in an 'umbrella-like' fashion. From this point on the reaction coordinate a much more substantial change in metal coordination geometry occurs as the H···Co separation decreases from ca. 2.4 to 2.2 Å resulting in a geometry best represented by the structure of **5**. At this point the metal coordination geometry (at least in terms of the carbonyl and phosphine ligands) already closely resembles that of the final product, namely the metal hydride (viz. L_{eq}–Co–L_{eq} 115.6 and L_{ax}–Co–L_{eq} 102.3 in **5** versus L_{eq}–Co–L_{eq} 117.3 and L_{ax}–Co–L_{eq} 99.7° in **17**). Thus, at this stage of the reaction one could argue that the metallate anion has adopted a geometry consistent with receiving the proton in the final stage of the reaction in which it is transferred to the metal, i.e. it is now 'prepared' for proton transfer.

It is noticeable that, with the exception of **4**, to which we will return shortly, no structures are represented in this last stage of the reaction for in which M–H separations lie in the range 2.2–1.6 Å. This observation is consistent with the report by Norton, Sweany and co-workers that hydrogen-bonded structures of the type $(CO)_4Co$–H···NR_3 are not formed [6]. Indeed our own efforts to prepare systems with shorter Co···H separations than in **5** by using trialkylphosphines have resulted in the formation of cobalt hydride species [24]. In this light, Midollini's N–H···Ni hydrogen-bonded structure, **4**, warrants further examination. Firstly the hydrogen atom appears to be primarily located on the nitrogen, based upon the X-ray crystal structure, though a refined N–H distance of 1.15(9) Å suggests a more weakened N–H bond relative to the preceding N–H···Co cases, and thus a stronger H···M interaction. The cage-like geometry of the $(Ph_2PCH_2CH_2)_3NH^+$

tripod ligand (Hnp_3^+) restricts the metal coordination geometry leading to the unusual situation in which the H···Ni separation is extremely short, but the metal geometry is still tetrahedral (both L_{eq}–Co–L_{eq} and L_{ax}–Co–L_{eq} have average values of 109.5°). The data point for **4** clearly lies well off the most probable reaction pathway, but illustrates that in such constrained systems very short N–H···M hydrogen bonds can be achieved even when the d^{10} metal center is not suitably 'prepared' for proton transfer [25]. The Structure Correlation study clearly demonstrates that **4** is a remarkable structure.

The structures of **11** and **12** also represent geometries that lie slightly off the main reaction pathway. Specifically they can be described as having a larger distortion away from tetrahedral geometry at the metal than anticipated given their Co···H separations. In the case of **11**, this makes sense in view of the much greater steric bulk of the cation relative to the ammonium groups used (e.g. $(DABCO)H^+$) in the other examples. For **12**, such an argument is not as strong. However, it should be noted that this structure is not just a simple binary system linked through an N–H···Co hydrogen bond. Rather is a five component hydrogen-bonded chain consisting of two outer $Co(CO)_4^-$ anions, each of which is linked to a central *N*-methylpiperazine molecule via an N–H···Co hydrogen bond and an N–H···N hydrogen bond, each originating from the secondary ammonium center of an *N*-methylpiperazinium cation.

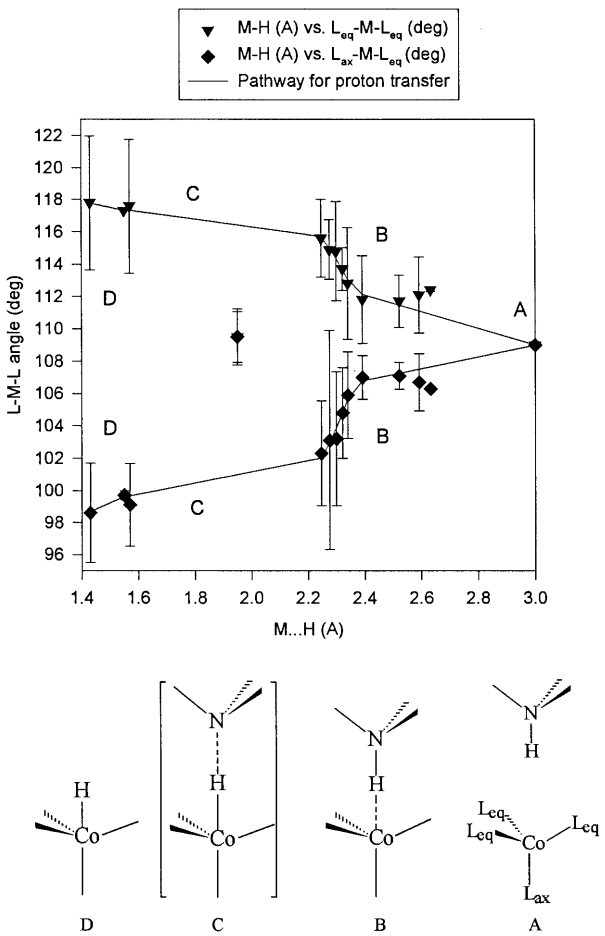

Fig. 3. Structure Correlation study, modelling the pathway for protonation of $Co(CO)_3L^-$ anion at the metal center. Error bars on L–M–L angles at 1σ level (see Scheme 1 for calculation of σ).

4. Summary

The low temperature X-ray crystal structure of an elusive organometallic zwitterion containing an intramolecular N–H···Co (d^{10}) hydrogen bond has been reported together with one of the common byproducts of its synthesis. A Structure Correlation study has been undertaken to derive a geometric model for the reaction pathway for protonation of the $Co(CO)_3L^-$ anion to yield the hydride complex $HCo(CO)_3L$ anion (L = CO, PR_3).

5. Supplementary material

Crystallographic data for the structural analyses have been deposited with the Cambridge Structural Data Centre, CCDC nos. 141607 and 141608 for compounds **2** and **3**, respectively. Copies of the information may be obtained free of charge from The Director, CCDC, 12 Union Road, Cambridge CB2 1EZ, UK (fax: +44-1223-336033; e-mail: deposit@ccdc.cam.ac.uk or www: http://www.ccdc.ca.ac.uk).

Acknowledgements

Financial support from the Donors of the Petroleum Research Fund, administered by the American Chemical Society, the Missouri Research Board, and an UMSL Research Award, is acknowledged. J.C.M.R. acknowledges further support in the form of fellowships from the UM-St. Louis Chemistry Alumni, the UM-St. Louis Graduate School and Mallinkrodt Chemical Co. We thank Mr Michael Groaning for the synthesis of the $Ph_2PCH_2CH_2NEt_2$ ligand. Purchase of the Bruker (Siemens) SMART diffractometer was funded in part by NSF grant no. CHE-9309690.

References

[1] G.R. Desiraju, T. Steiner, The weak hydrogen bond, in: IUCr Monographs on Crystallography, No. 9, Oxford University Press, Oxford, 1999.

[2] (a) T. Steiner, Crystallogr. Rev. 6 (1996) 1. (b) G.R. Desiraju, Acc. Chem. Res. 24 (1991) 270. (c) G.R. Desiraju, Acc. Chem. Res. 29 (1996) 441. (d) R. Taylor, O. Kennard, J. Am. Chem. Soc. 104 (1982) 5063.

[3] (a) L. Brammer, J.M. Charnock, P.L. Goggin, R.J. Goodfellow, A.G. Orpen, T.F. Koetzle, J. Chem. Soc. Dalton Trans. (1991) 1789. (b) L. Brammer, M.C. McCann, R.M. Bullock, R.K. McMullan, P. Sherwood, Organometallics 11 (1992) 2339. (c) L. Brammer, D. Zhao, Organometallics 13 (1994) 1545. (d) L. Brammer, D. Zhao, F.T. Ladipo, J. Braddock-Wilking, Acta Crystallogr. Sect. B 51 (1995) 632. (e) D. Zhao, F.T. Ladipo, J. Braddock-Wilking, L. Brammer, P. Sherwood, Organometallics 15 (1996) 1441. (f) L. Brammer, J.C. Mareque Rivas, D. Zhao, Inorg. Chem. 37 (1998) 5512. (g) J.C. Mareque Rivas, L. Brammer, Coord. Chem. Rev. 183 (1999) 43. (h) L. Brammer, in: J.A.K. Howard, F.H. Allen, G.P. Shields (Eds.), Implications of Molecular and Materials Structure for New Technologies, Kluwer, Dordecht, The Netherlands, 1999, pp. 197–210.

[4] (a) F. Calderazzo, G. Fachinetti, F. Marchetti, P.F. Zanazzi, J. Chem. Soc. Chem. Commun. (1981) 181. (b) F. Cecconi, C.A. Ghilardi, P. Innocenti, C. Mealli, S. Midollini, A. Orlandini, Inorg. Chem. 23 (1984) 922. (c) I.C.M. Wehman-Ooyevaar, D.M. Grove, H. Kooijman, P. van der Sluis, A.L. Spek, G. van Koten, J. Am. Chem. Soc. 114 (1992) 9916. (d) I.C.M. Wehman-Ooyevaar, D.M. Grove, P. de Vaal, A. Dedieu, G. van Koten, Inorg. Chem. 31 (1992) 5484. (e) S.G. Kazarian, P.A. Hamley, M. Poliakoff, J. Am. Chem. Soc. 115 (1993) 9069. (f) A. Albinati, F. Lianza, B. Müller, P.S. Pregosin, Inorg. Chim. Acta 208 (1993) 119. (g) A. Albinati, F. Lianza, P.S. Pregosin, B. Müller, Inorg. Chem. 33 (1994) 2522. (h) Y.S. Shubina, L.M. Epstein, J. Mol. Struct. 265 (1992) 367. (i) E.S. Shubina, A.N. Krylov, A.Z. Kreindlin, M.I. Rybinskaya, L.M. Epstein, J. Mol. Struct. 301 (1993) 1. (j) E.S. Shubina, A.N. Krylov, A.Z. Kreindlin, M.I. Rybinskaya, L.M. Epstein, J. Mol. Struct. 465 (1994) 259. (k) D. Braga, F. Grepioni, E. Tedesco, K. Biradha, G.R. Desiraju, Organometallics 16 (1997) 1846. (l) Y. Gao, O. Eisenstein, R.H. Crabtree, Inorg. Chim. Acta 254 (1997) 105. (m) G. Orlova, S. Scheiner, Organometallics 17 (1998) 4362. (n) J. Kozelka, J. Bergès, R. Attias, J. Fraitag, Angew. Chem. Int. Ed. 39 (2000) 198.

[5] (a) This is not to say that there are no examples of bona fide M–H···A hydrogen bonds (for examples, see Refs. [5b–f]). Such cases have been characterized, but these typically involve cationic metal hydrides, in which the positive charge associated with the hydrogen bond donor may compensate for the fact that the hydrogen–metal bond is polarized $M^{\delta+}$–$H^{\delta-}$. An unusual case is the neutral intramolecular hydrogen bond reported by Pickett and co-workers [5d]. (b) M.A. Adams, K. Folting, J.C. Huffman, K.G. Caulton, Inorg. Chem. 18 (1979) 3020. (c) L.M. Epstein, E.S. Shubina, A.N. Krylov, A.Z. Kreindlin, M.I. Rybinskaya, J. Organomet. Chem. 447 (1993) 227. (d) S.A. Fairhurst, R.A. Henderson, D.L. Hughes, S.K. Ibrahim, C.J. Pickett, J. Chem. Soc. Chem. Commun. (1995) 1569. (e) E. Peris, R.H. Crabtree, J. Chem. Soc. Chem. Commun. (1995) 2179. (f) D. Braga, F. Grepioni, E. Tedesco, K. Biradha, G.R. Desiraju, Organometallics 15 (1996) 2692.

[6] Either no hydrogen bond is formed or proton transfer occurs to give A–H^+ and $Co(CO)_4^-$. See, S.S. Kristjánsdóttir, J.R. Norton, A. Moroz, R.L. Sweany, S.L. Whittenburg, Organometallics 10 (1991) 2357.

[7] P. Sherwood, L. Brammer, unpublished results.

[8] (a) K.P. Klein, C.R. Hauser, J. Org. Chem. 32 (1967) 1479. (b) T.B. Rauchfuss, F.T. Patino, D.M. Roundhill, Inorg, Chem. 14 (1975) 652.

[9] SHELXTL-5.0, Bruker Analytical X-ray, Inc., Madison, WI, USA 1995.

[10] G. Sheldrick, SABABS, version 2, University of Göttingen, 1995.

[11] R.H. Blessing, Acta Crystallogr. Sect. A 51 (1995) 33.

[12] The H···Co distance and N–H···Co angle are calculated by extending the N–H distance along the determined N–H vector to a value of 1.054 Å, as determined by neutron diffraction for $Et_3NH^+Co(CO)_4^-$ [3b]. For **2**, as the ammonium hydrogen could not be located in the difference map, the N–H vector was also calculated, assuming sp^3 hybridization at nitrogen.

[13] In **5** and **6**, the $(DABCO)H^+$ cation is disordered over two orientations, the minor orientation being eclipsed (C–N···Co–C ca. 0°) rather than staggered with the anion. Furthermore the structure of $(Quinuclidine)H^+Co(CO)_4^-$ exhibits an ordered eclipsed geometry about the hydrogen bond [3f].

[14] (a) This is particularly well documented for L = CO, where decomposition has been shown to be autocatalytic resulting from the presence of $^{\bullet}Co(CO)_4$ radicals [14b]. (b) R.W. Wegman, T.L. Brown, J. Am. Chem. Soc. 102 (1982) 2494.

[15] (a) F.W.B. Einstein, R. Kirkland, Acta Crystallogr. Sect. B 34 (1978) 1690. (b) J.A. Ibers, J. Organomet. Chem. 14 (1968) 423. (c) R.A. Jones, M.H. Seeberger, A.L. Stuart, B.R. Whittlesey, T.C. Wright, Acta Crystallogr. Sect. C 42, (1986) 399. (d) T. Bartik, B. Bartik, B.E. Hanson, K.H. Whitmire, I. Guo, Inorg. Chem. 32 (1993) 5833. (e) P. Braunstein, D.G. Kelly, Y. Dusausoy, D. Bayeul, M. Lanfranchi, A. Tiripicchio, Inorg. Chem. 33 (1994) 233. (f) D.H. Farrar, A.J. Lough, A.J. Poe, T.A. Stromnova, Acta Crystallogr. Sect. C 51 (1995) 2008.

[16] (a) H.-B. Bürgi, J.D. Dunitz, Acc. Chem. Res. 1983, 16, 153. (b) H.-B. Bürgi, J.D. Dunitz (Eds.), Structure Correlation, VCH, Weinheim, Germany, 1993.

[17] E.A. MacNeill, F.R. Scholer, J. Am. Chem. Soc. 99 (1977) 6243.

[18] L.S. Leigh, K.S. Whitmire, Acta Crystallogr. Sect. C 45 (1989) 210.

[19] M.B. Smith, R. Bau, J. Am. Chem. Soc. 95 (1973) 2388.

[20] A preliminary version of Figure 3 has appeared in slightly different form in Ref. [3h].

[21] L. Brammer, M.C. McCann, R.M. Bullock and R.K. McMullan, unpublished results for neutron structure at 123 K. See also Ref. [3b] for report of neutron structure at 15 K.

[22] E.J. Moore, J.M. Sullivan, J.R. Norton, J. Am. Chem. Soc. 108 (1986) 2257.

[23] A.J. Bondi, J. Chem. Phys. 68 (1964) 441.

[24] D. Zhao, L. Brammer, unpublished results.

[25] (a) Some may have cause to question the assignment of an N–H···Ni hydrogen bond in **4**. However, spectroscopic data (^{1}H-NMR δ 14.5 N–H and IR ν(N–H) 2130 cm^{-1} br) and computational results (EHMO) support this assignment. Perhaps most convincing is the N···Ni separation in **4** at 3.092(8) Å is substantially shorter than in the deprotonated analog $(np_3)Ni(CO)$ at 3.25(1) Å [24b]. (b) C.A. Ghilardi, A. Sabatini, L. Sacconi, Inorg. Chem. 15 (1976) 2763.